

White-Light Emission from Annealed ZnO:Si Nanocomposite Thin Films.

Shabnam^a, Chhaya Ravi Kant^a and P. Arun^{b*}

^aDepartment of Applied Sciences,
Indira Gandhi Institute of Technology,
Guru Gobind Singh Indraprastha University,
Delhi 110 006, India.

^bDepartment of Physics & Electronics,
S.G.T.B. Khalsa College,
University of Delhi, Delhi - 110 007, India

October 8, 2018

Abstract

As grown ZnO:Si nanocomposites of different compositional ratios were fabricated by thermal evaporation techniques. These films were subjected to post deposition annealing under high vacuum at a temperature of 250C° for 90min. The photoluminescence (PL) spectra of annealed samples have shown marked improvements both in terms of intensity and broadening. For the first time in ZnO:Si nanocomposite films we see huge UV, red and orange peaks at 310, 570 and 640nm. Structural and Raman analysis show formation of a Zn-Si-O shell around ZnO nano clusters wherein on heating Zn₂SiO₄ compound forms. The new emissions are due to Zn₂SiO₄ which completes white light spectrum.

Keywords Nano-composites, Nanostructures, Photoluminescence, Oxides

*email:arunp92@physics.du.ac.in, Telephone:091 011 29258401, Fax: 091 011 27666220

1 Introduction

Ever since the extraction of blue light from Mg doped Gallium Nitride(GaN) was made possible, research has been directed to yield cost effective white light emitting devices from a single chip. Owing to its structural similarity with GaN and wide band gap of $\sim 3.2\text{eV}$ ZnO is considered as a promising candidate for white-light production [1, 2]. In this direction, ZnO based nanostructures and nanocomposites have received ample attention. ZnO based nanocomposites have gained more importance in the field of white light emission. This is because an appropriate host material not only aids in broadening of light emission but also gives stability to the film by preventing agglomeration of the ZnO grains. To this effect, Silicon becomes a preferred choice to be used as host species [3, 4, 5]. This is because of the central role played by Silicon in the microelectronic industry and its known emissions in red region in its nanophase.

For obtaining cost-effective white light, Klason et al [6] have deposited n-type ZnO nanorods on p-Si. The films emitted white light on forward biasing. Depositing of ZnO nanoparticles in porous silicon (po-Si) has also been reported by Bo et al [7] and Singh et al [8]. Researchers like Pal [9] and Peng et al [10] had studied the effect of varying ZnO to Silicon content obtained by RF sputtering. Preliminary investigations taken up by our group have reported discrete UV, blue, green and weak red wavelengths from ZnO:Si nanocomposites grown by vacuum thermal evaporation technique [11, 12]. It was also seen that an improvement took place in the luminescence emission of the samples by subjecting them to post deposition heat treatment [13]. Post deposition treatments have been reported to bring variations in Photoluminescence spectra profile by other research groups as well [9, 14, 15]. In this manuscript we report the systematic study carried out to investigate the influence of annealing on ZnO:Si nanocomposites with varying ZnO:Si compositional ratio.

2 Experimental

ZnO:Si nanocomposites films were fabricated by thermally evaporating a mixture of powdered ZnO and n-Silicon at a vacuum of $\sim 10^{-6}$ Torr in a Hind High Vac (Bengaluru), Thermal evaporation coating unit, Model 12A4D. The deposition was carried out on microscopic glass substrates maintained at room temperature. Starting material was prepared by mixing ZnO and Silicon in the proportions of 1:1, 1:2, 1:3, 2:3 and 2:5 (by weight). These mixtures were then pelletized, to prevent its flying off the boats. As deposited nanocomposite films were subjected to annealing under high vacuum of the order of $\sim 10^{-6}$ Torr and then allowed to cool naturally under vacuum. Films of varying composition with thickness 600\AA are named as sample (a1), (b1), (c1), (d1) and (e1) in order of the increasing Silicon content in starting material. The vacuum annealed counterparts are referred to as (a1v), (b1v), (c1v), (d1v) and (e1v).

The structural studies of the surface is measured by Pananalytical PW3050/60 Grazing Incidence angle X-Ray Diffractometer (GIXD) and that of the bulk region by Philips PW 3020 X-Ray Diffractometer (XRD). X-Ray Photoelectron Spectroscopy (XPS) was performed with Perkin-Elmer X-ray Photo-electron Spectrometer (Model 1257) with Al $K\alpha$ (1486 eV) X-ray source. Photoluminescence (PL) scans were recored on Fluorolog Jobin Yvon spectroscope (Model 3-11) using an excitation wavelength of 270nm. Renishaw's "Invia Reflex" Raman spectroscope was used for measurements using Ar^{+2} . The surface morphology and texture of the as grown nanocomposite films were studied using TECHNAI-20 G^2 Transmission Electron Microscope (TEM). Below we enlist the results of the various analysis done on our samples.

3 Results and Discussion

3.1 X-Ray Diffraction & Chemical Composition Studies

3.1.1 Structural Study

The structural changes in the films caused by heat treatment was examined using GIXD. To compare the effect of heat-treatment, Figure 1(A) and 1(B) shows the GIXD scans of the samples after fabrication and post vacuum annealing. Similar to the pattern obtained for the as grown films, the GIXD scans of the annealed samples show peaks at $2\theta=36^\circ$ and 43° . These peaks are the (101) and (102) plane of ZnO and Zn respectively. A mixed response is seen on heat treatment with no variation in samples (b1v) and (e1v), however, there is a marked increase in peak intensities in (d1v) while it diminishes in (c1v).

To investigate the increase in peak intensity of sample (d1v), we have calculated the grain size of the pre and post annealed samples. The grain size as calculated from the ZnO peak of (d1) was 8.7nm while that of sample (d1v) was found to be 9.9 ± 3 nm. This marginal or no change in grain size was evident in the other samples also. No growth in grain/cluster size is not surprising since the ZnO nano-clusters are embedded in Silicon matrix which would deter any further agglomeration.

3.1.2 Chemical Composition

The surface and the film's bulk are usually different [12] and hence it is necessary to investigate the film below the surface. For this we studied the samples using XPS not only at the surface but also beneath it by sputtering 125Å of film layer. Figure 2(A) shows this depth profiling, recorded for Zn-2p_{3/2} of sample (c1v). Presence of a single peak at around 1022eV suggests Zinc exists in the sample as ZnO. Contribution from elemental Zinc if any is insignificant. However, a shift to higher binding energy along the film thickness is visually evident from figure 2(A) (and plotted in figure 3A). Before proceeding, it is worth mentioning that the existence of single Silicon peak in XPS as is the case with Oxygen (figure 2B and 2C respectively) eliminates the possibility of existence of elemental Zinc and Silicon dioxide through out the film.

In our previous report on as deposited films, we had observed that Zinc's 2p_{3/2} peak shift towards lower energy side along the film thickness. We believe this shift is related to the change in the neighboring environment in terms of relative ZnO to Silicon abundance. However, here we see a shift in Zinc's peak towards the higher energy side as we move deeper into the film.

Following the methodology we adopted in our earlier work [12], we determined the ratio of ZnO to Si along the thickness of the film. Figure 3(B) shows the linear decrease of this ratio with film depth. Decrease in ZnO:Si ratio from 1.023 to 0.271 along the depth of the film can also be interpreted as an increase in the Silicon content with the depth of the film. Combining the results of Figure 3(A) and 3(B), figure 3(C) shows the variation of ZnO peak position with ZnO:Si ratio. The data indicates a shift in Zinc 2p_{3/2} peak to the lower energy side with decreasing Silicon environment. Though the samples under study here and in our previous study were different, the fact that Zinc 2p_{3/2} peak moves to the lower energy side with decreasing Silicon environment is consistent. Thus, structurally, morphologically and compositionally vacuum annealing has not effected our sample.

3.2 Raman Spectra

We have noticed that Raman spectra reveals more information on the structural properties of our nano-composites than X-Ray diffraction [12]. Hence, to investigate the structural modification incorporated in our samples on vacuum annealing we analysed the samples using Raman spectroscopy. The Raman spectra was taken in standard back scattering geometry using Argon ion laser for excitation. Figure 4 compares the Raman spectra of the as grown samples (a1-e1) with their vacuum annealed counterparts (a1v-e1v). The as grown films irrespective of the ZnO/Si starting ratio gave broad spectra in 300-600cm⁻¹ range. The spectras were

essentially three prominent unresolved peaks, namely at $\sim 310, 440$ and 565 cm^{-1} . The $\sim 310\text{cm}^{-1}$ peak corresponds to the LA mode of amorphous Silicon [11, 12]. Similarly, the $\sim 440\text{cm}^{-1}$ and $\sim 565\text{cm}^{-1}$ peaks are attributed to Wurtzite ZnO bond vibrations and defect related bondings in ZnO respectively [17, 18].

Visual examination show significant changes not only in peak sizes but also in their positions. For example, the plot of figure 5(A) shows variation in ratio of area enclosed by the 440cm^{-1} peak of the vacuum annealed sample to that of as grown with ZnO content. A decreasing trend is seen with increasing ZnO content. We believe that this decrease manifests due to decrease in ordering in the ZnO. Also, the ordering is easily broken in samples with higher ZnO content on vacuum annealing. Even the peak position (440cm^{-1}) of the annealed samples as compared to those of as deposited peaks show a linear trend with the peak moving to a higher wave-number on annealing (fig 5B). That is, on vacuum annealing the peak position corresponding to bondings of the Wurtzite structured ZnO shows increased wave-number where the increase is more substantial if the as grown samples peak was at a higher wave number. This too must be indicative of increased disorder. Also, Yadav et al [19] have reported an increase in wavenumber with decreasing grain size. This would reason that vacuum annealing has resulted in a decrease in grain size (except for sample a1v).

This lack of ordering discussed above should reflect in the vacuum annealed sample's $\sim 565\text{cm}^{-1}$ peak that corresponds to the defects in ZnO [20]. Plots of Δ_{VA}/Δ_{AG} (Δ represents peak area of vacuum annealed 'VA', and as grown 'AG') and I_{VA}/I_{AG} (peak intensities) with varying ZnO content shows linear trend. Figure 5(C) shows the variation in ratio of intensities with ZnO content. As expected, the linear trend with positive slope suggests an increase in the defects in vacuum annealed ZnO:Si nanocomposites for samples with large ZnO content. There also data point of 'd1v' stands apart from the trendline. However, this indicates 'd1v' contains appreciable defects along with substantial ordering. The fact that sample 'd1v' shows a simultaneous increase in crystallinity and defects appears contradictory at first glance, however, we have been able to show that a sample with comparable amounts of defects co-existing with good ordering gives broadening in PL spectra [12]. Figure 6 gives a plot of relative presence of Wurtzite ZnO to ZnO with defects ($\Delta_{438\text{cm}^{-1}}/\Delta_{565\text{cm}^{-1}}$) with varying ZnO content. This graph helps in predicting broadening of PL spectra. In an earlier work on as grown samples (shown by filled circles in figure 7), it was observed that samples which had nearly equal areas (and hence ratio ~ 1) showed maximum broadening in PL [12]. It can be appreciated from the plot that the sample 'd1v' has nearly equal areas of the peaks resulting from defect free and defect related ZnO lattices. Moreover, sample 'd1v' lies on the minimum of the curve (visual aid showing the trend), so it is expected to show maximum broadening in photoluminescence. The downward shift of the 'a1v' data point shows that this sample has also got comparable contributions from wurtzite and defect related ZnO structures. As per our prediction, 'a1v' should also show broadening in PL spectra along with the other heat treated samples.

Finally we now comment on the reduction in the $\sim 310\text{cm}^{-1}$ peak of annealed samples as compared to that in the as deposited samples. In our ZnO:Si nanocomposites, we have ascribed this peak to LA mode of amorphous Silicon [11, 12]. Since the annealing of the samples has been done in the high vacuum of the order of 10^{-6} torr, as also by our XPS results we rule out the possibility of Silicon's oxidation. Hence, we believe this reduction is due to some improvement in ordering of Silicon. However, since XRD failed to give a nanocrystalline peak of Silicon, we believe only short-range ordering of amorphous silicon has taken place.

3.3 Photoluminescence Spectra

In our previous works we have shown that a broad spectra is achievable from ZnO:Si nanocomposite films. However, they had poor or no emission in the red wavelength region. To obtain further broadening and to improve emission in the red wavelength region, we annealed our samples under high vacuum. Figure 7 compares the PL spectra of samples (a1) and (a1v). Broadening accompanied with a multifold increase in intensity on annealing can be easily appreciated. In the absence of prominent shoulders resulting from broadening of peaks we were not able to deconvolute the spectra using standard softwares. However, based on our knowledge from study of asgrown samples we expect peaks at 365 and 420nm. These peaks correspond to band edge emission from Wurtzite ZnO and the interfacial layer between ZnO grains and Si background. These two peaks in the

annealed samples were unresolved and hence using Peakfit-4 we have placed a peak at 395nm (fig 8). In the previous section, Raman analysis suggested a decrease in the grain size of ZnO accompanied with reduction in 438cm^{-1} peak implying decrease in Wurtzite ordering. A direct relationship between the Raman 438cm^{-1} peak and PL's 365nm was established [12]. Thus one expects a reduced contribution from the band edge emission peak of ZnO. However, since the unresolved peak remains significant, one can infer an improvement in contribution from the interface, i.e. the 420nm peak. Another peak of the blue region which appears in asgrown samples and persists even after annealing is the 470nm peak. We attribute this peak too to the interface [10, 12].

Increasing ZnO content in this study showed decreasing grain size, hence the 430nm peak seems to be enhanced for samples with smaller grain size. A question that would need answering would be "*how can diminishing grain size contribute more to an emission process?*". To analyse this we took a sample (this sample was used in our earlier study [13]) and heated it at 250°C for intervals of 30, 60, 120min. The grain size was found to decrease with increased heating. We had proposed the formation of a "shell" around the increasingly crystalline ZnO with Zn-Si-O shell material growing into the asgrown cluster, thus reducing the grain size. In fig 8 we plot the PL 430nm peak with increasing shell volume. Shell volume V_{shell} is

$$V_{\text{shell}} \propto R_o^3 - R_n^3$$

where, R_o is the grain size of the as grown sample and R_n is that of annealed samples. We find a linear co-relation, suggesting that the 430nm PL emission peak intensity is due to the "shell" volume or in turn amount of Zn-Si-O linkages present.

The PL spectra was recorded without use of optical filters. This results in the presence of a huge peak at 540nm which is called the second harmonic peak. As compared to the unheated samples PL spectra, the neck of this harmonics is quite broad (example fig 6). This broadening maybe due to existence of the 540nm green peak associated with oxygen vacancy in ZnO. While this peak was resolvable in as grown sample's PL spectra from the second harmonic peak, we were not able to do the same in this study.

The other two peaks lying at 570nm and 640nm with marked contributions have been observed for the first time in our samples. While 570nm peak could be ascribed to emission between energy levels caused by Zn interstitial defects [21] it does not explain the existence of the 640nm peak. Contribution of emission from nano-Si can be ruled out as per our XRD and Raman analysis. We believe vacuum annealing has transformed some of the ZnO and Si linkages present in the shell into Zn_2SiO_4 . Zn_2SiO_4 is known to emit strongly in red, orange and UV regions [22, 23]. In fact one can notice the UV emission at 310nm is strong whenever an intense 570 and 640nm emission peak exists. We noticed that the sample (c1v), which has significant red and orange emissions also show a huge 310nm peak.

Discussion

Based on our previous studies and results from the present work, we now are in a position to explain the processes taking place in ZnO:Si nanocomposite films. While the Silicon matrix prevents ZnO grains from agglomerating the unsaturated bonds of ZnO and Si at the interface form Zn-Si-O linkages. The interface thus contributes to emissions at 420nm and 470nm. Due to the thermal evaporation technique used for fabrication, ZnO clusters have defects. While the ordered bondings give rise to emissions at 350nm, those associated with defects give emissions at 540nm. based on relative proportion of the two, the contribution of emission varies. We have shown comparable proportions give comparable emissions and has a broadening of PL in the blue-green region. Annealing results in migration of defects from the core of ZnO to the interface. This results in increased Zn-Si-O bondings that go on forming a shell which expands inwards decreasing ZnO grain size. Appropriate temperature of annealing leads to the formation of Zn_2SiO_4 within the shell that leads to new emissions in UV and red regions. As stated the present work along with our initial results give a good insight of

the material process taking place and gives scope of understanding how to engineer samples for broad emission white light LEDs based on ZnO:Si nanocomposites.

Conclusion

As deposited nanocomposites of ZnO:Si of various compositional ratios were annealed under high vacuum. Structural and compositional studies carried out by X-Ray Diffraction and XPS were not able to detect appreciable variation. However, PL spectra have shown a significant improvement. Not only have the intensities increased but appearance of three new peaks at 310, 570 and 620nm can be easily noticed. These peaks appeared along with earlier reported peaks in the blue-green region. Annealing has not only pushed the interface into the ZnO grain but also transformed Zn-Si-O linkages present at interface into Zn_2SiO_4 . We attribute the new peaks to Zn_2SiO_4 existing in the shell surrounding the ZnO grains. This study further substantiates our earlier claims correlating broadening in blue-green region to existence of appropriate ratio of two phase, namely crystalline and defect related ZnO. Sample (a1v) shows improved broadening as compared to its as grown counterparts, due to appropriate mix of the two phases achieved after annealing in vacuum. Presence of all the wavelengths completes our white-light spectrum. We thus successfully show that suitable ZnO:Si compositional ratio with appropriate post deposition treatment is crucial for obtaining white light. This study along with more careful investigations should pave the way for future white light emitting devices

Acknowledgment

We are thankful to Dr.D.K.Pandaya at Indian Institute of Technology, Delhi for GIXD measurements. The resources utilized at University Information Resource Center, Guru Gobind Singh Indraprasta University is gratefully acknowledged. We also would like to express our gratitude to Dr. Kamla Sanan and Dr. Mahesh Sharma (both at National Physical Lab., Delhi) for carrying out the photoluminescence and XPS studies respectively. Author CRK is thankful to University Grants Commission (India) for financial assistance in terms of research award, F.No-33-27/2007(SR). One of the authors PA is grateful to Department of Science and Technology (India) for funding present work with research project SR/NM/NS-28/2010. .

Figure Captions

1. GIXD scans of (A) as grown and (B) vacuum annealed samples.
2. XPS depth profile scans of (A) $2p_{3/2}$ peaks of Zinc (B) Silicon and (C) Oxygen of sample (c1v).
3. (A) Variation of Peak position of Zn $2p_{3/2}$ with depth (B) Fraction of Zinc in bonding to amount of Silicon present along the thickness and (C) Peak position of Zinc in bonding with Oxygen to its fraction of presence.
4. Raman spectra of (A) as grown samples (a1), (b1), (c1), (d1), (e1) and (B) vacuum annealed samples (a1v), (b1v), (c1v), (d1v) and (e1v). Also seen are the deconvoluted peaks assigned to amorphous silicon (310cm^{-1}), wurtzite structure of ZnO (438cm^{-1}) and with defect related peak of ZnO (570cm^{-1}).
5. (A) Relative change in Intensity of 438 cm^{-1} peak in vacuum annealed samples to that in as grown samples with respect to zno content, (B) Variation of peak position in the 438 cm^{-1} peak in vacuum annealed samples with respect to that in the as grown samples and (C) Relative change in Intensity of 560 cm^{-1} peak in vacuum annealed samples to that in as grown samples with respect to ZnO content.
6. Relative presence of defect related ZnO to wurtzite ZnO (Area 438cm^{-1} /Area 565cm^{-1} from Raman Spectra) for varying ZnO content in film for (A) vacuum annealed (B) as deposited films.
7. PL spectra of samples (a1) and (a1v). (Counts of (a1) have been scaled by 3 (i.e.X3) to compare the spectra.)
8. PL of samples (a1v), (b1v), (c1v) and (d1v).
9. Plot of shell volume with respect to intensity of 430nm observed in photoluminescence (method described in the text).

References

- [1] C. Jagadish and S. J. Pearton, “Zinc Oxide Bulk, Thin Films and Nanostructures, Elsevier Ltd.”, 2006.
- [2] U. Ozgur, Ya. I. Alivov, C. Liu, A. Teke, M. A. Reshchikov, S. Dogan, V. Avrutin, S.-J. Cho and M. Morkoc, *J. Appl. Phys.*, **98** (2005) 041301 (and the references therein).
- [3] A.K.Das, P.Misra and L.M.Kukreja, *J.Phys. D:Appl. Phys.*,**42** (2009) 165405.
- [4] B.Yang, A.Kumar, H.Zhang, P.Feng, R.S.Katiyar and Z.Wang, *J.Phys. D:Appl. Phys.*,**42** (2009) 045415.
- [5] W.J.Shen, J.Wang, Q.Y. Wang, Y.Duan and Y.P. Zheng, *J.Phys. D:Appl. Phys.*,**39** (2006) 269.
- [6] P. Klason, P. Steegstra, O. Nur, Q-H. Hu, M. M. Rahman, M. Willander and R. Turan, *Proceedings: “ENS 2007, Paris: France (2007)”*.
- [7] ZHAO Bo, LI-Q-S, Qi H-X and ZHANG N, *Chin Phys.Lett.*, **23** (2006) 1299.
- [8] R. G. Singh, Fouran Singh, V. Aggarwal and R. M. Mehra, *J.Phys. D: Appl. Phys.*, **40** (2007) 3090.
- [9] U. Pal, J. Garcia Serrano, N. Koshizaki and T. Sasaki, *Mater. Sci. Eng. B*, **113** (2004) 24.
- [10] Yu-Yun Peng, Tsung-Eong Hseih and Chia-Hung Hsu, *Nanotechnology*, **17** (2006) 174.
- [11] S.Siddiqui, C.R.Kant, P.Arun and N.C.Mehra. *Phys. Lett. A* **372** (2008) 7068.
- [12] Shabnam, C.R.Kant and P.Arun. *Size and Defect related Broadening of Photoluminescence Spectra in ZnO:Si Nanocomposite Films.* communicated available at arXiv:1007.2142.
- [13] Shabnam, C.R.Kant and P.Arun. *Mater. Res. Bull.* **45** (2010) 13068.
- [14] Z.D.Sha, Y.Yan, W.X.Qin, X.M.Wu and L.J.Zhuge, *J.Phys. D:Appl.Phys.* **39** (2006) 3240.
- [15] H.S.kan, J.S. Kang, S.Sik Pang, E.S.Shim and S.Y.Lee, *Mater. Sci. and Engg. B* **102** (2003) 313.
- [16] “ *Elements of X-Ray Diffraction*”, B.D.Cullity (London,1959)
- [17] Ramon Cusco, Esther Alarcon-Llado, Jordi Ibanez, Luis Artus, Juan Jimenez, Buguo Wang, and Michael J. Callahan, *Phys. Rev. B* **75** (2007) 165202.
- [18] K.A.Alim, V.A.Fonoberov and A.A.Balandin, *J.Appl.Phys.*, **97** (2005) 124313.
- [19] H.K.Yadav, V.Gupta, K.Sreenivas, S.P.Singh, B.Sundrakannan and R.S.Katiyar, *Phys. Rev. Lett.*,**97** (2006) 085502.
- [20] C.X.Xu, X.W.Sun, B.J.Chen, P.Shum, S.Li and X.Hu, *J.Appl.Phys.*,**95** (2004) 661.
- [21] N.Bano, I.Hussain, O.Nur, M. Willander, P.Klason and A.Henry, *Semicond.Sci.Technol.*,**24** (2004) 125015.
- [22] Q.Zhuang, X.Feng, Z.Yang, J.Kang and X.Yuan, *Appl. Phys. Lett.*, **93** (2008) 091902.
- [23] X.Feng, X.Yuan, T.Sekiguchi, W.Lin and J.Kang, *J.Phys.Chem. B*, **109** (2005) 15786.

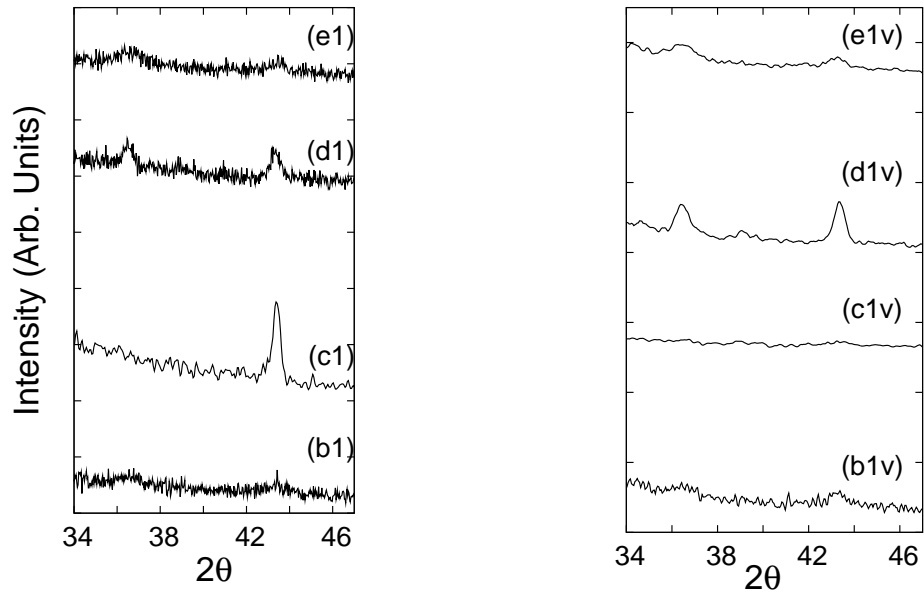


Figure 1: GIXD scans of (A) as grown and (B) vacuum annealed samples.

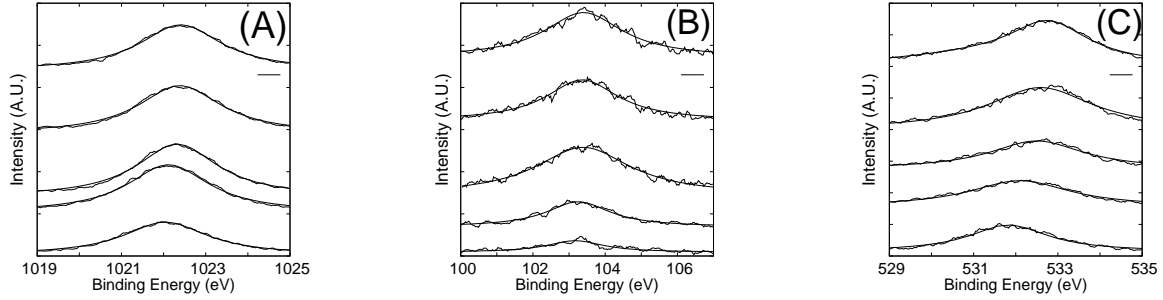


Figure 2: XPS depth profile scans of (A) $2p_{3/2}$ peaks of Zinc (B) Silicon and (C) Oxygen of sample (c1v).

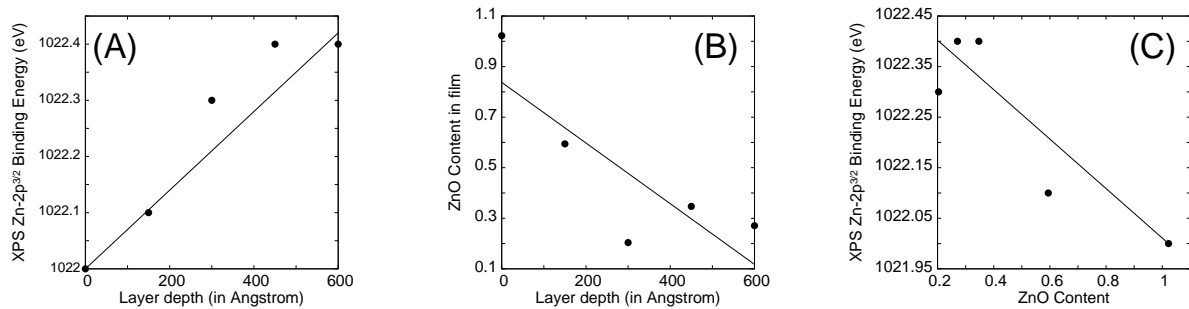


Figure 3: (A) Variation of Peak position of Zn 2p_{3/2} with depth (B) Fraction of Zinc in bonding to amount of Silicon present along the thickness and (C) Peak position of Zinc in bonding with Oxygen to its fraction of presence.

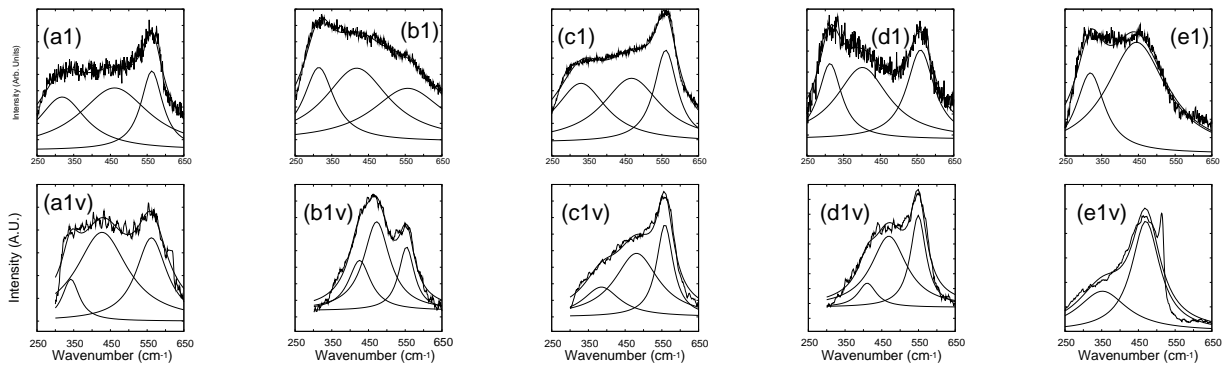


Figure 4: Raman spectra of (A) as grown samples (a1), (b1), (c1), (d1), (e1) and (B) vacuum annealed samples (a1v), (b1v), (c1v), (d1v) and (e1v). Also seen are the deconvoluted peaks assigned to amorphous silicon (310cm⁻¹), wurtzite structure of ZnO (438cm⁻¹) and with defect related peak of ZnO (570cm⁻¹).

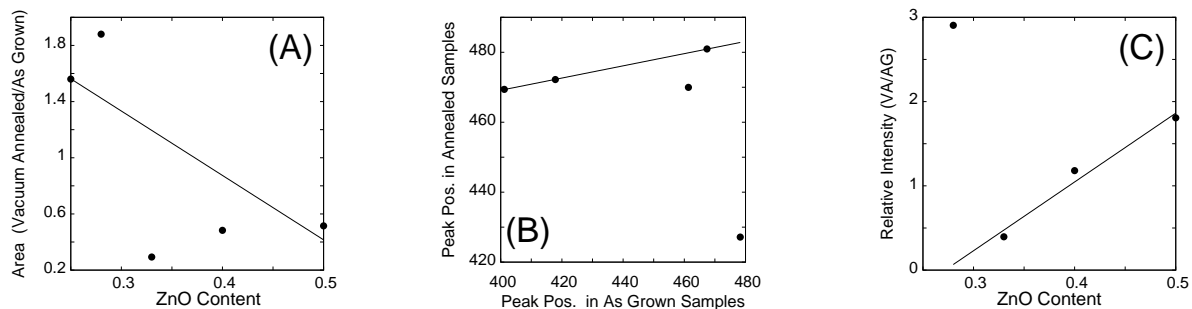


Figure 5: (A) Relative change in Intensity of 438 cm⁻¹ peak in vacuum annealed samples to that in as grown samples with respect to zno content, (B) Variation of peak position in the 438 cm⁻¹ peak in vacuum annealed samples with respect to that in the as grown samples and (C) Relative change in Intensity of 560 cm⁻¹ peak in vacuum annealed samples to that in as grown samples with respect to ZnO content.

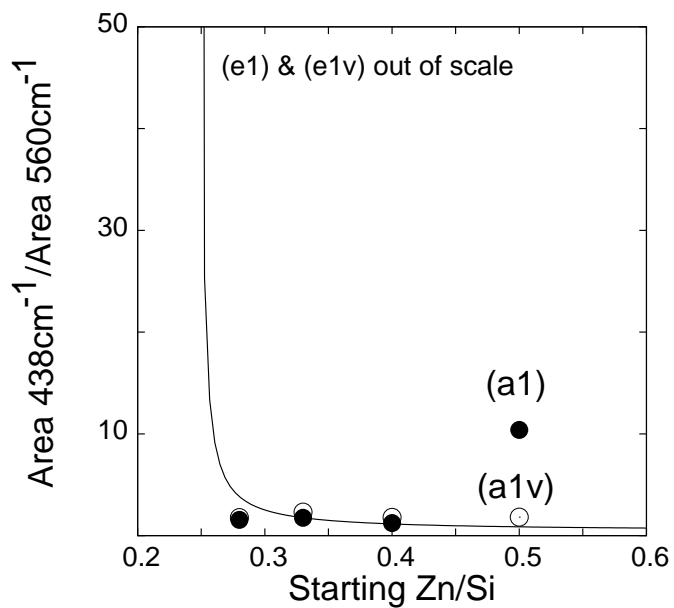


Figure 6: Relative presence of defect related ZnO to wurtzite ZnO ($\text{Area } 438\text{cm}^{-1} / \text{Area } 565\text{cm}^{-1}$ from Raman Spectra) for varying ZnO content in film for (A) vacuum annealed (B) as deposited films.

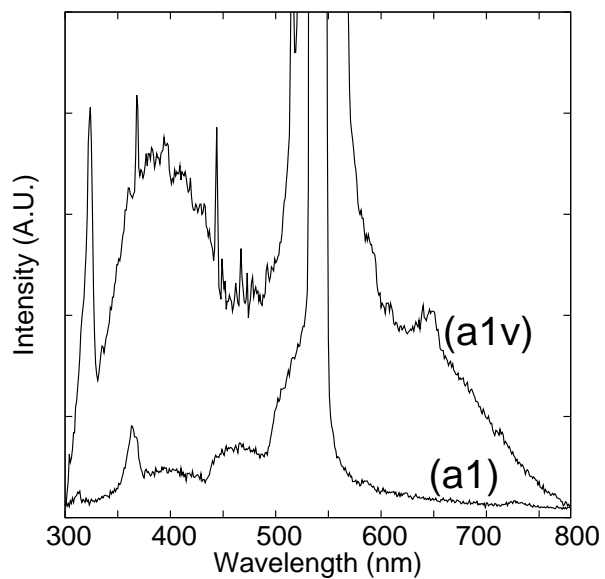


Figure 7: PL spectra of samples (a1) and (a1v). (Counts of (a1) have been scaled by 3 (i.e. X3) to compare the spectra.)

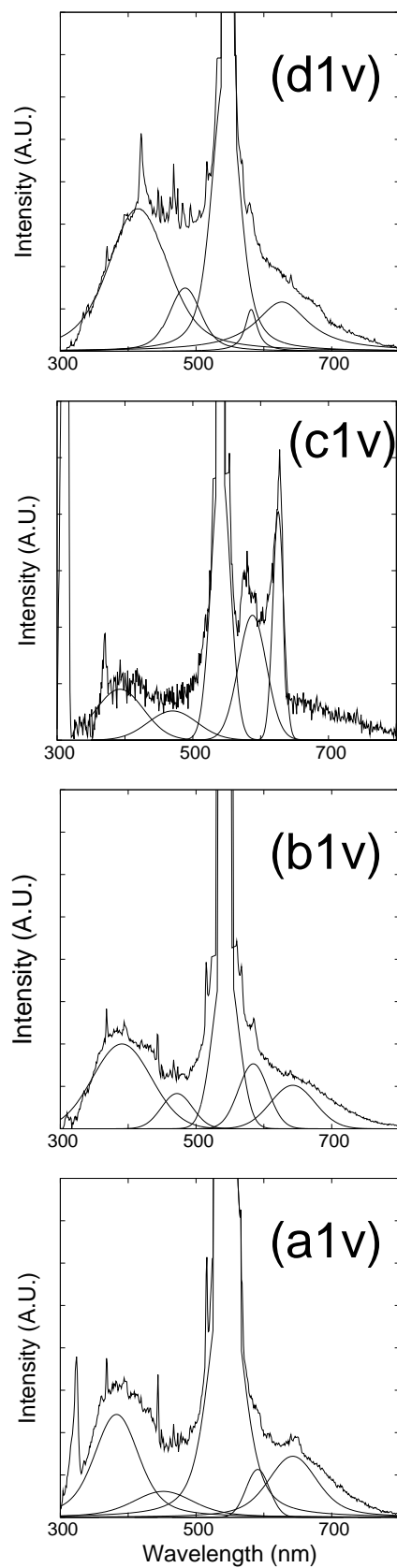


Figure 8: PL of samples (a1v), (b1v), (c1v) and (d1v).

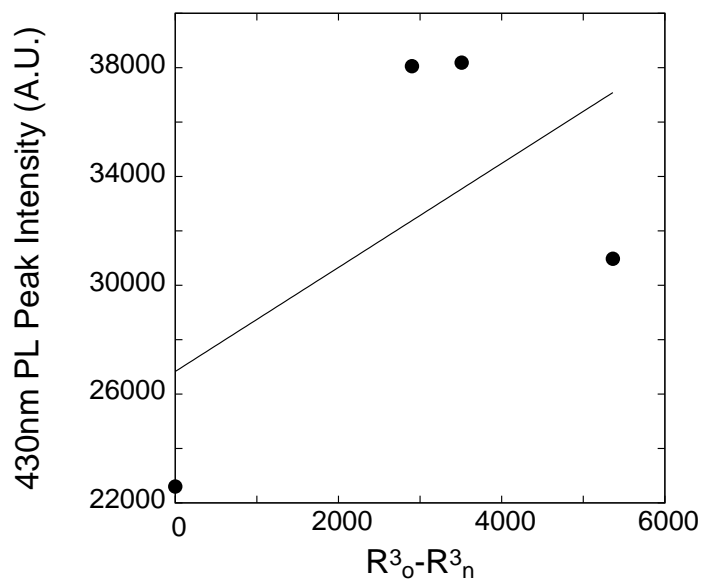


Figure 9: Plot of shell volume with respect to intensity of 430nm observed in photoluminescence (method described in the text).